

PERGAMON

Deep-Sea Research II 48 (2001) 1837–1863

DEEP-SEA RESEARCH
PART II

www.elsevier.com/locate/dsr2

A predictive model for estimating rates of primary production in the subtropical North Pacific Ocean

Michael E. Ondrusek*, Robert R. Bidigare, Kirk Waters[1], David M. Karl

Department of Oceanography, University of Hawaii, Honolulu, HI 96822, USA

Abstract

A primary production model, specific to the subtropical North Pacific, was developed using productivity and chlorophyll data collected at Station ALOHA (22.75°N, 158.00°W) and measured phytoplankton physiological parameters. The production algorithm is a mechanistic, full spectral model that provides depth-dependent photosynthesis rates. Six years of phytoplankton pigment data were analyzed to derive seasonal cycles and to parameterize chlorophyll *a* (Chl; monovinyl and divinyl chlorophyll *a*) versus depth profiles. The Chl profiles fit a Gaussian-type distribution with depth over a constant background concentration equal to mixed-layer values. Maximum Chl concentrations were always found below the surface, and the parameters displayed distinct monthly and seasonal patterns. Photosynthesis versus irradiance experiments were conducted at a number of locations and seasons in the vicinity of Station ALOHA to calculate phytoplankton physiological parameters needed for the computation of primary production rates. Relationships were explored between environmental conditions and the physiological and profile parameters in order to develop algorithms based on remotely sensed sea-surface variables and time of year. These relationships were used to model primary production rates using data collected during the Hawaii Ocean Time-series (HOT) program. The performance of the model and model parameters were tested by comparing modeled results to those measured directly at Station ALOHA by trace metal-clean, in situ ^{14}C incubation techniques. Monthly averaged chlorophyll profile parameters and a constant maximum quantum yield ($0.026\,mol\,C\,(mol\,quanta)^{-1}$) generates an annual production estimate of $168\,g\,C\,m^{-2}$, which closely resembles that measured at Station ALOHA ($181\,g\,C\,m^{-2}$) during the same period. The measured and modeled primary production rates for the subtropical North Pacific are twice as high as values derived from Coastal Zone Color Scanner (CZCS) data ($60–90\,g\,C\,m^{-2}$) during the period 1978–1986. If the study area near Station ALOHA is representative of most oligotrophic waters, current global estimates of primary production rates have been significantly underestimated. © 2001 Elsevier Science Ltd. All rights reserved.

* Corresponding author. Present address: NOAA Science Center, Camp Springs, MD 20746, USA.
E-mail address: mondrusek@resdis.noaa.gov (M.E. Ondrusek).
[1] Presently at NOAA Coastal Services Center, Charleston, SC 29405, USA.

0967-0645/01/$ - see front matter © 2001 Elsevier Science Ltd. All rights reserved.
PII: S0967-0645(00)00163-6

1. Introduction

Modeling primary production rates with a high degree of precision in oligotrophic oceanic waters is difficult due to the relatively narrow range and low concentrations of surface Chl compared to more dynamic and productive regions (Prézelin et al., 1987; Bidigare and Ondrusek, 1996; Behrenfeld and Falkowski, 1997). A nutricline persistently deeper than the mixed-layer depth limits surface mesoscale variability (Winn et al., 1995) and the separation of nutrient-replete deep waters from the nutrient-deplete mixed-layer results in nearly constant and low surface Chl concentrations (Ondrusek et al., 1991; Letelier et al., 1996). Deeper in the water column, there is a "bell-shaped" deep chlorophyll maximum layer (DCML) centered at or immediately above the nutricline. The two-layer vertical structure of the euphotic zone complicates this modeling effort as deeper processes may be decoupled from the surface (Letelier et al., 1996). Increases in primary production as a result of nutrient injections from below may not always be manifested by increases in surface Chl. When modeling phytoplankton parameters using remote sensing data, processes occurring below the sea surface must be parameterized using environmental variables (e.g., SST or sea-surface height anomaly) or by time of year. Consequently, it is difficult for models to account for the relatively high variance observed for direct production estimates (Sorensen and Siegel, 2001).

The Hawaii Ocean Time-series (HOT) program has made repeated measurements of a variety of key biogeochemical processes at a benchmark station approximately 100 km north of Oahu, Hawaii. The HOT database spans more than a decade (1988–present) and is an excellent resource for assessing seasonal and interannual processes that either regulate or are related to primary production rates. This database also provides a means of testing the predictability of bio-optical production models. Relationships developed from data collected at Station ALOHA (22.75°N, 158.00°W) should be representative of the oligotrophic gyre due to the absence of strong spatial gradients in physical and biogeochemical characteristics. This is reflected in phytoplankton populations that can maintain horizontally homogenous distributions at the group level for thousands of kilometers (e.g. Venrick, 1971, 1990; Ondrusek et al., 1991).

With the launch of the Sea-viewing Wide Field-of-view Sensor (SeaWiFS), ocean-color data are once again available for the global ocean for estimating near-surface Chl concentrations. The primary goal of this study is to develop a remote sensing algorithm for estimating integral and depth-dependent primary production rates in the North Pacific Subtropical Gyre (NPSG) from satellite-measured near-surface Chl concentrations ($Chl_{[sat]}$) and incident solar radiation. Combining accurate local primary production estimates from different regions also improves and aids global carbon modeling efforts required to trace the fate of anthropogenically produced carbon dioxide.

Primary production rates at depth in the upper 200 m were predicted using a full spectral, absorption-based model. Efforts were focused on predicting phytoplankton photo-physiological parameters and Chl concentrations below the remote sensing depth. The time series of primary production rates measured at Station ALOHA enabled the identification of relevant seasonal patterns, and along with the measurements of phytoplankton physiological parameters, the development of a NPSG-specific primary production algorithm. This algorithm yields production estimates that are consistent with measured rates and are approximately two-fold higher than those based on previous CZCS imagery (Antoine et al., 1996; Behrenfeld and Falkowski, 1997; Longhurst et al., 1995).

2. Methods

The algorithm presented here was developed to produce maps of integral primary production for the NPSG. The principal input parameters for the production model are sea-surface $Chl_{[sat]}$ derived from SeaWiFS ocean-color data, and surface E_{PAR} computed from the International Satellite Cloud Climatology Project (Bishop et al., 1997). Phytoplankton photo-physiological parameters, as well as sub-surface values of Chl and irradiance, cannot be measured via satellites and must be estimated based on climatological and experimental data. Constant values with respect to time and space can be used or they can be adjusted through parameterization via a dynamic model. The HOT data base (1988–present) and measurements made in conjunction with the Marine Optical BuoY (MOBY) project (Hooker et al., 1992) have been analyzed for relationships that can be employed to improve production models.

2.1. Primary production equation

This model was developed to predict ocean primary production rates at depth based on satellite observations and utilized the following equation from Bidigare et al. (1987):

$$P_z = 12{,}000\ (\mathrm{mg\,C\,mol\,C^{-1}})\Phi_c E_{abs}, \tag{1}$$

where P_z is the instantaneous primary production rate ($\mathrm{mg\,C\,m^{-3}\,h^{-1}}$) at depth z, the constant 12,000 converts mol C into mg C, Φ_c is the in situ quantum yield of photosynthesis ($\mathrm{mol\,C\,(mol\,quanta)^{-1}}$), and E_{abs} is the absorbed quanta by phytoplankton ($\mathrm{mol\,quanta\,m^{-3}\,h^{-1}}$). A time and depth grid of production is made using Eq. (1). For this exercise we utilized 10 equal time intervals from 0600 to 2000 h and calculated production at depth every 5 m from 0 to 200 m for each time interval. Daily production estimates ($\mathrm{mg\,C\,m^{-2}}$) are then calculated by integrating the discrete estimates with respect to depth and time throughout the day.

2.2. E_{abs}

The quanta available to be absorbed by phytoplankton are a function of surface irradiance and the propagation of this irradiance through the water column. The parameterization of E_{abs} is accomplished by decomposing the solar irradiance into spectral components via the 5S radiative transfer code (Tanré et al., 1990) and propagating the spectral light field through the ocean using two stream approximations with published absorption and scattering coefficients and Chl concentrations at depth. The surface spectral and temporal light field is calculated based on location and time of year using the Tarné model. The spectral surface values for each time of day are normalized to match the total measured daily irradiance. All the absorption and scattering coefficient calculations used to propagate the light through the water column are performed spectrally and then integrated over the range of the photosynthetically available radiation (E_{PAR}, 400–700 nm). Phytoplankton absorption is determined as a function of wavelength and Chl concentration according to Morel (1988) or Bricaud et al. (1995). Absorption by colored dissolved organic matter a_{cdom} is determined as a function of Chl concentration according to Prieur and Sathyendranath (1981).

2.3. Quantum yield

Φ_c is parameterized based on maximum quantum yield and the available light at depth (Jassby and Platt, 1976; Bidigare et al., 1992):

$$\Phi_c = \Phi_{max} E_k E_{PAR}^{-1} \tanh(E_{PAR} E_k^{-1}), \quad (2)$$

where E_k (μmol quanta $m^{-2} s^{-1}$) is the saturation parameter for photosynthesis and E_{PAR} (μmol quanta $m^{-2} s^{-1}$) is the photosynthetically available radiation. The $E_k E_{PAR}^{-1}$ ratio is parameterized as a log function of E_{PAR} according to Waters et al. (1994), and E_k is measured directly via photosynthesis versus irradiance (P versus E) experiments. Φ_{max} (mol C (mol quanta)$^{-1}$) is the maximum quantum yield of photosynthesis, and is computed using the equation

$$\Phi_{max} = \alpha \overline{a_{ph}^{-1}}, \quad (3)$$

where α (mol C m^{-3}) (mol quanta m^{-2})$^{-1}$ is the light-limited rate of photosynthesis determined from P versus E curves, and $\overline{a_{ph}}$ is the spectrally weighted phytoplankton absorption coefficient (m^{-1}). Values of $a_{ph}(\lambda)$ were estimated by spectral reconstruction using HPLC-measured pigment concentrations (Bidigare et al., 1990) and also by the filter-pad technique (Kishino et al., 1985). Φ_{max} was assumed to be constant throughout the day and with depth unless otherwise specified.

2.4. P versus E experiments

In 1996 and 1997, during four separate cruises, P versus E experiments were conducted aboard the R/V *Moana Wave* in the vicinity of Station ALOHA (Fig. 1). P versus E measurements (Schofield et al., 1990; Ondrusek and Bidigare, 1997) along with simultaneous measurements of primary production (Letelier et al., 1996), HPLC pigment concentrations (Wright et al., 1991; Goericke and Repeta, 1993), and phytoplankton absorption (Kishino et al., 1985; Bidigare et al., 1990) were determined. The majority of the data was collected during three cruises near the MOBY mooring site off of Lanai [MOBY cruises, 157.0°W, 20.8°N, September 1996 ($n = 3$), November 1996 ($n = 13$), and February 1997 ($n = 8$)] and the remainder of the data was collected during a Station ALOHA to Station CLIMAX transect [ACT cruise, July 1996 ($n = 24$); Ondrusek and Bidigare, 1997]. During each cruise, P versus E and simulated in situ production measurements (in situ measurements also were performed during the ACT cruise) were made daily throughout the euphotic zone, using clean techniques (Fitzwater et al., 1982).

The time series of P versus E experiments along with $a_{ph}(\lambda)$ measurements conducted at the HOT and MOBY locations are used to describe the variability and identify patterns in the maximum rate of photosynthesis (P_{max}), α, E_k, and Φ_{max}. To measure the P versus E responses of natural phytoplankton populations, four photosynthetrons (cf. Lewis and Smith, 1983) were constructed. For each sample, twenty-eight 20-ml borosilicate scintillation vials were filled with seawater and spiked with approximately 425 kBq of ^{14}C sodium bicarbonate. Duplicate sub-samples of the stock ^{14}C solution were collected before each experiment to determine the activity of the tracer added. Two vials were processed for initial (T_0) counts, and two control vials were incubated in the dark. The tracer uptake in the dark controls was subtracted from the P versus E rates to correct for dark

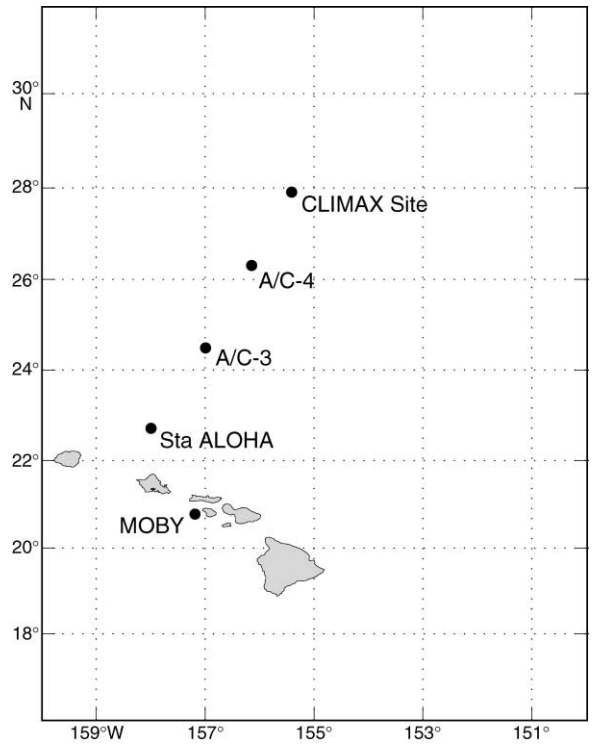


Fig. 1. Map of the study area identifying Station ALOHA, the CLIMAX Site, and the MOBY Site.

uptake. The remaining samples were incubated under 24 different light levels in one of four identical photosynthetrons.

Each photosynthetron was illuminated with two 250 W tungsten halogen lamps (Vantage Lighting, CA). The light beam passed through a heat shield gel (ROSCO thermashield) to remove infra-red light and then through a 2.54-cm thick layer of a saturated copper sulfate solution, producing a spectral quality of light that, although shifted to the red, as near as possible resembled the near-surface in situ light field while maintaining saturating light levels (Fig. 2). After the copper sulfate solution, the beam of light passed through neutral density filters, producing 24 different levels of photosynthetically available radiation (E_{PAR}, 0–2000 μmol quanta $m^{-2} s^{-1}$). Light entered the samples through the bottom of the scintillation vials set in black aluminum cooling blocks. The upper mixed-layer samples were cooled using pumped surface seawater. The two deeper samples were cooled to in situ temperatures with a refrigerated water bath. Samples were incubated for 1 h. The spectral quality of the light was measured with a SpectraScope fiber optic probe attached to an S1000 spectrometer (Ocean Optics, Inc.). E_{PAR} was measured in each sample well prior to each experiment with a Biospherical QSL-100 PAR meter. The start time was defined as the time when the lamps were switched on, and the stop time was defined as the time when the lamps were switched off. Each 22-ml sample was filtered through a 25-mm glass fiber filter (GF/F), acidified with 1 ml of 10% HCl for 24 h and then fixed with 10 ml of Aquasol II (Dupont, Inc.). The activities of the samples were counted initially and then recounted two to four weeks later. The later counts were used in the calculations (Letelier et al., 1996).

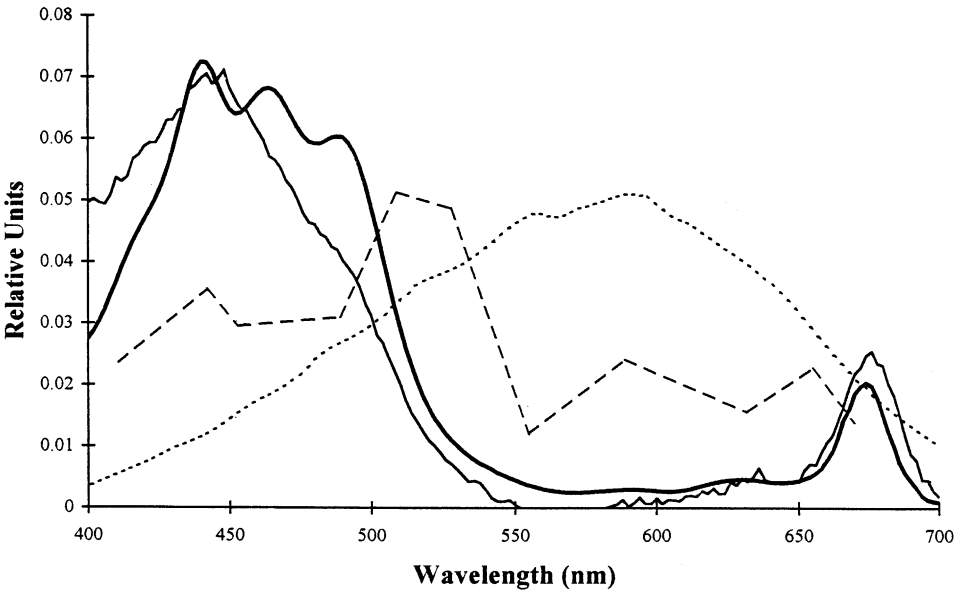


Fig. 2. Spectral irradiance properties used in the calculation of phytoplankton physiological parameters. (1) Absorption by phytoplankton ($m^2\,mg\,Chl^{-1}$) estimated via spectral reconstruction using HPLC-measured phytoplankton pigments (solid line; Bidigare et al., 1990); (2) absorption by phytoplankton ($m^2\,mg\,Chl^{-1}$) measured by the filter-pad technique (thin solid line; Kishino et al., 1985); (3) average full spectral irradiance output (E; $\mu mol\,m^{-2}\,s^{-1}\,nm^{-1}$; full scale = 0–8.0 $\mu mol\,m^{-2}\,s^{-1}\,nm^{-1}$) for the photosynthetron (dotted line); and (4) downwelling irradiance (E_d; $\mu mol\,m^{-2}\,s^{-1}\,nm^{-1}$; full scale = 8.0 $\mu mol\,m^{-2}\,s^{-1}\,nm^{-1}$) measured just below the surface near the MOBY Site on 15 July 1997 (dashed line).

P versus E curves were defined by the data points using a non-linear, best-fit solution to Eq. (4). Eq. (4) is based on Jassby and Platt (1976) with a photoinhibition term (Neale and Richerson, 1987):

$$P^{b} = P^{b}_{max}\tanh(E_{PAR}E_{k}^{-1})^{-\beta(E_{PAR}-E_{t})} \quad (4)$$

P^{b}_{max} is the Chl-specific maximum rate of photosynthesis ($mg\,C\,mg\,Chl^{-1}\,h^{-1}$) and E_k is the saturation parameter for photosynthesis (μmol quanta $m^{-2}\,s^{-1}$). The expression $-\beta(E_{PAR}-E_t)$ is a photoinhibition term, where β is the negative slope of the P versus E curve encountered under high light levels and E_t is the light level at the onset of photoinhibition. The phytoplankton physiological parameters were then determined from the P versus E curves (Fig. 3). Values of P^{b}_{max} and E_k were determined by fitting the data using Eq. (4), and α (for use in Eq. (3)) was calculated as $P^{b}_{max}E_{k}^{-1}$.

2.5. Chlorophyll a profiles

Chl profiles were parameterized using the equation given in Lewis et al. (1983) and modified by Platt et al. (1988):

$$b_z = b_o + \left(\frac{h}{\sigma\sqrt{2\pi}}\right)\exp\left(-\frac{(z-z_m)^2}{2\sigma^2}\right), \quad (5)$$

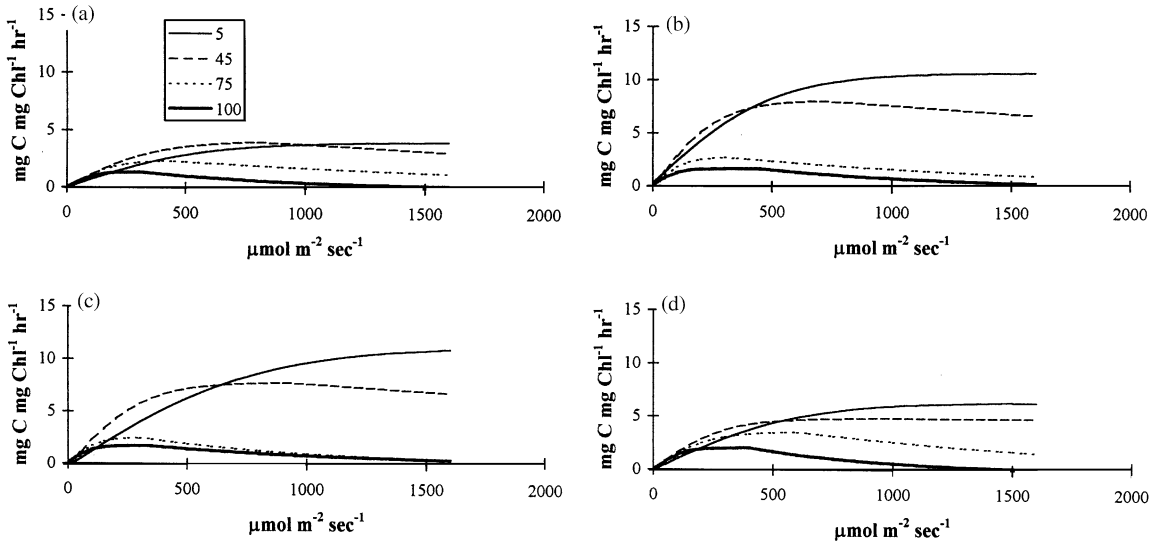


Fig. 3. Modeled photosynthesis versus irradiance curves calculated from data collected on the ACT cruise from Station ALOHA to the CLIMAX Site during July 1996. P versus E curves are predicted from data fits using Eq. (6). (a) A/C-2; Station ALOHA, 22.75°N, 158.00°W. (b) A/C-3; 24.57°N, 157.00°W. (c) A/C-4; 26.38°N, 156.17°W. (d) A/C-5; CLIMAX Site, 28.00°N, 155.41°W.

where b_z is Chl at depth z ($\mu g\,m^{-3}$), b_o is the background, mixed-layer Chl concentration ($\mu g\,m^{-3}$), σ is the standard deviation of the width of the Chl maximum peak (m), h is the integrated Chl above b_o ($\mu g\,m^{-2}$), and z_m is the depth of the Chl maximum layer (m) (Fig. 4). HPLC-determined Chl profiles from Station ALOHA (1989–1995) were fit using Eq. (5). The Gaussian parameters were binned by month and season, and linear regressions of h, σ, z_m, and a were run against b_o to identify patterns and relationships that might be useful for describing Chl profiles for remote sensing applications. Temporal means and regression relationships were then used to reconstruct Chl profiles using only time and $Chl_{[sat]}$.

2.6. Model parameter evaluation

2.6.1. Chl(z)

To evaluate errors associated with parameterizing Chl profiles by a Gaussian distribution, and to analyze our ability to predict profiles for modeling primary production from satellite observations, simulations were run using the full spectral model (FSM) with data from HOT cruises 23–68 (1991–1995). Chl profiles were described by (1) holding $Chl_{[sat]}$ (surface Chl concentrations measured fluorometrically from production casts; Letelier et al., 1996) constant with depth; (2) using Gaussian parameters calculated for a given cruise from pigment data obtained during the HPLC cast (different cast from that used to measure production); (3) using $Chl_{[sat]}$ for b_o and average monthly σ, h, and z_m to reconstruct Chl(z); (4) using the fluorometrically measured Chl profile from the production cast for each cruise; (5) using $Chl_{[sat]}$ for b_o and average σ, h, and z_m for reconstructing Chl(z); and (6) using the average fluorometrically measured Chl profile from the production casts (all cruises).

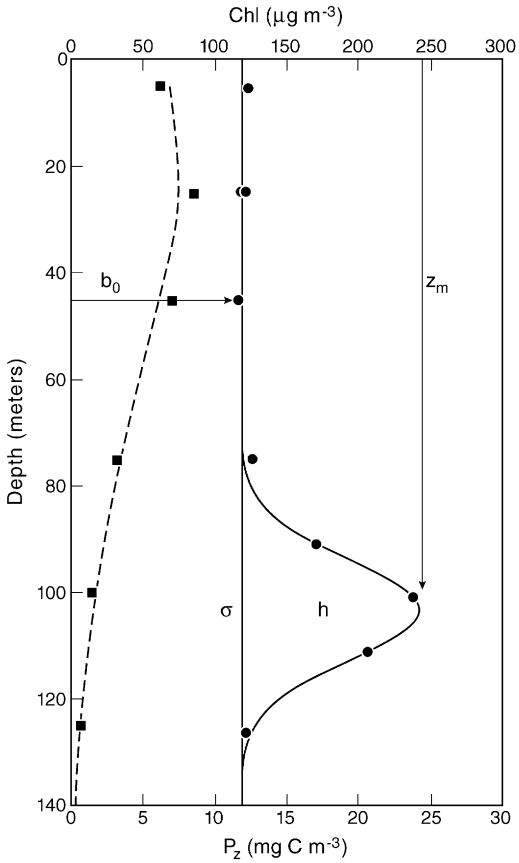


Fig. 4. Chl profile measured (●) and modeled (solid line) from HOT cruise 27, collected on 7 December 1991. The modeled curve is a best fit to Eq. (7). Measured (■) versus modeled (dashed line) in situ primary production is also compared for the same cruise.

2.6.2. E_k

In addition to testing different Chl parameterizations, the FSM was applied to HOT data while varying E_k, Φ_{max}, and the phytoplankton absorption coefficient. E_k in Eq. (2) takes the form of a ratio: $E_k E_{PAR}^{-1}$. For the default value in the FSM, the ratio $E_k E_{PAR}^{-1}$ is described as a function of E_{PAR} (Waters et al., 1994) and therefore varies as a function of depth and time of day. In addition, a time- and depth-varying E_k was tested. The latter was averaged from P versus E experiments from the ACT and MOBY cruises and held constant between cruises when modeling the HOT data. The third and fourth E_k parameterizations used an E_k value held constant with depth and time of day, but varied between cruises as a function of surface Chl because relationships to $Chl_{[sat]}$ are most desirable when using satellite-based models. Linear regressions of Chl(z) with volumetric P_{max} and α values (0–45 m) had r^2 values of 0.853 and 0.841, respectively (Table 1). These relationships were used to calculate P_{max} and α from $Chl_{[sat]}$ values (1991–1995) for HOT cruises 23–68 and, subsequently, these values were used to calculate E_k for each cruise. The specific E_k value for each cruise was then held constant with respect to depth (0–200 m) and time of day to calculate Φ_c (Eq. (2)) in the production estimates shown in Fig. 9a.

Table 1
Results of least squares linear regression analyses between phytoplankton physiological parameters and HPLC-determined Chl concentrations from P versus E experiments conducted during the ACT and MOBY cruises (N = number of observations)

Parameter	r^2	Slope	Intercept	N
α (0–45 m)	0.841	0.028	− 0.001	30
P_{max} (0–45 m)	0.853	7.534	− 0.216	30
E_k (0–100 m)	0.458	− 1671	562	45
a_{ph} (0–75 m)	0.928	0.012	0.000	40
Φ_{max} (0–100 m)	0.674	0.151	0.005	41

To analyze errors associated with spectral differences between the photosynthetron and the in situ light fields, the E_k values modeled as a function of $Chl_{[sat]}$ were adjusted to in situ values based on the relationship between E_k values spectrally weighted to the in situ irradiance field and those determined directly in the photosynthetron during the ACT cruise (E_k in situ = (E_k photosynthetron) (0.463) − 27.938; $r^2 = 0.941$, $n = 8$). To accomplish this, Φ_{max} was multiplied by $\overline{a_{ph}}$ (calculated with knowledge of Chl-specific a_{ph}, the in situ light field (Fig. 2), and the Chl concentration) to obtain a value of in situ α. In situ E_k was computed by dividing P_{max}, which is spectrally independent above saturating light levels, by the in situ α. On average, in situ α was 3.6 times greater than α measured in the photosynthetron, and in situ E_k was 0.40 times smaller than the E_k measured in the photosynthetron. The HOT $Chl_{[sat]}$-dependent E_k values determined above were then adjusted to in situ values and tested in the full spectral model (Fig. 9b).

2.6.3. $E_{PAR}(z)$

To test how light attenuation affects the accuracy of the FSM, different published $a_{ph}(\lambda)$ values were utilized (Morel, 1988; Bricaud et al., 1995). In addition, average Chl-specific $a_{ph}(\lambda)$ values were determined via the filter-pad absorption technique, with and without detrital absorption (Kishino et al., 1985), and by spectral reconstruction of HPLC pigment data (Bidigare et al., 1990) collected on the ACT cruise. Absorption by colored dissolved organic matter (a_{cdom}) was modeled using the method of Prieur and Sathyendranath (1981). The sensitivity of the model to this additional absorption was tested by excluding a_{cdom}. Sensitivity of the model to detrital absorption also was evaluated.

3. Results

The default method for the FSM was the Bricaud et al. (1995) parameterization for $a_{ph}(\lambda)$, a constant Φ_{max} value of 0.03 mol (C mol quanta)$^{-1}$ (Ondrusek and Bidigare, 1997), an E_{PAR}-dependent E_k parameterization for estimating Φ_c (Waters et al., 1994), and measured Chl profiles (Table 2). Performance of the FSM in predicting depth-dependent primary production rates was

Table 2
Mean daily primary production ($P_{200\,m}$; g C m^{-2}) for 1991–1995 at Station ALOHA calculated using the full spectral model (10 calculations between 0600 and 2000 h, 41 depths) and results of model II regression analyses between measured and modeled $P_{200\,m}$. The mean measured daily $P_{200\,m}$ at Station ALOHA for the cruises used in the model comparisons was 0.510 g C m^{-2}

Parameter	Mean	r[a]	Slope	Intercept	n
Default method[b]	0.528	0.713	0.569	0.248	31
Constant Chl	0.481	0.530	0.452	0.258	31
HPLC Gaussian profile	0.507	0.513	0.473	0.274	31
$Chl_{[sat]}$ and Gaussian profile[c]	0.536	0.607	0.501	0.289	31
$Chl_{[sat]}$ + average Gaussian	0.530	0.629	0.497	0.286	31
Average Chl profile	0.536	0.695	0.532	0.274	31
E_k weighted to incubator	1.060	0.712	1.451	0.346	31
E_k weighted to in situ	0.816	0.674	1.158	0.246	31
Average measured E_k	0.532	0.692	0.599	0.237	31
Average measured a_{ph}	0.555	0.705	0.612	0.255	31
Morel (1988) a_{ph}	0.443	0.691	0.513	0.190	31
Assume $a_{cdom} = 0$	0.649	0.727	0.691	0.309	31
Average filter pad a_{ph}	0.539	0.710	0.600	0.244	31
Average filter pad a_{ph} and a_p	0.597	0.698	0.647	0.279	31
$\Phi_{max} = 0.026$[d]	0.451	0.713	0.486	0.212	31
$\Phi_{max} = 0.028$[e]	0.490	0.713	0.566	0.218	31
Average Φ_{max}[f]	0.683	0.713	0.789	0.303	31
Φ_{max}, a_{ph}, and α regression	0.296	0.108	0.941	− 0.167	31
Φ_{max} from Chl regression	0.314	0.199	0.554	0.046	28

[a]Correlation coefficient.
[b]Bricaud et al. (1995) $a_{ph}(\lambda)$ parameterization, $\Phi_{max} = 0.030$, E_k/E_{PAR} parameterization of Φ_c (Waters et al., 1994) and measured Chl profiles.
[c]Surface Chl from productivity cast measured fluorometrically used for b_o. Monthly averages used for other Gaussian parameters.
[d]Average Φ_{max} for all stations.
[e]Φ_{max} value with best fit to measured data.
[f]Average depth- and time-dependent Φ_{max}.

evaluated by plotting modeled (default method) versus measured (Station ALOHA; 1991–1995) production rates (Fig. 5). No depth-dependent biases were observed, and 82% of the variance was explained by the FSM. A sensitivity analysis was performed by changing one variable at a time, with the goal of determining the best model parameterization for remote sensing applications in the NPSG. This exercise also evaluated the FSM's sensitivity to changes in variables and allowed identification of the critical variables that affect model performance.

3.1. Chlorophyll profiles

Chl below the remote sensing depth was specified by one of three methods: (1) input of measured Chl(z); (2) holding Chl constant with depth, and (3) modeling Chl profiles using Eq. (5). For remote

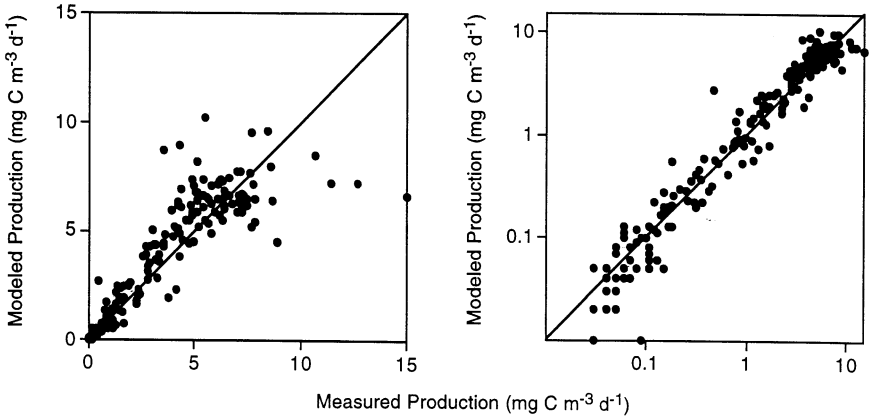


Fig. 5. Cross-plot of modeled daily primary production ($mg\,C\,m^{-3}\,d^{-1}$) versus measured daily primary production ($mg\,C\,m^{-3}\,d^{-1}$) from monthly data collected from Station ALOHA (1989–1995). Result of model II regression analysis is $Modeled_{0-200\,m} = 0.98 Measured_{0-200\,m} + 0.25$ ($r^2 = 0.82$, $n = 216$). Line is $x = y$. The data are also plotted in log–log space to examine model performance at low production rates.

sensing applications, constant Chl(z) or modeled Chl profiles must be utilized because only $Chl_{[sat]}$ is retrieved by the ocean-color measurements. Monthly averaged values for the coefficients b_o, σ, and h all display distinct seasonal patterns, while monthly averaged values of z_m remain relatively constant throughout the year (Fig. 6). The coefficients h, σ, and z_m all display minimum values during the winter months and maximum values in the summer months, and all are inversely related to b_o. Model predictions that used constant $Chl_{[sat]}(z)$ (Fig. 7a) and Gaussian parameters calculated from HPLC data from the same cruise (Fig. 7b) yielded the poorest predictions compared to measured production rates ($r = 0.530$ and 0.513, respectively; Table 2). Results from the simulations run with $Chl_{[sat]}$ substituted for b_o (Fig. 7c), average values of σ, h, and z_m (Fig. 7e) and average measured Chl profiles (Fig. 7f), most closely resembled predictions based on measured Chl profiles (Fig. 7d).

3.2. P versus E parameters

Depth-dependent and diurnal variations in photosynthetic parameters derived from P versus E experiments have been described previously for the equatorial Pacific (Cullen et al., 1992; Lindley et al., 1995) and for coastal regions of the North Pacific (Prézelin et al., 1987; Schofield et al., 1993). During this investigation, P versus E parameters displayed depth-dependent patterns that are consistent with photoadaptation (Fig. 8). P^b_{max} and E_k show a general pattern of decreasing in magnitude with increasing depth, while Φ_{max} and α^b generally increase in a depth-dependent fashion. During the ACT cruise, a diatom bloom was encountered at the two middle stations (A/C-3 and A/C-4; Fig. 1), providing the opportunity to sample "anomalous" conditions (cf. Ondrusek and Bidigare, 1997). At stations inside the diatom bloom, α^b and Φ_{max} values were highest at 45 m (Fig. 8b and d). One of the primary objectives of this study was to document the magnitude of these parameters in the NPSG for use in the FSM described above. Because P^b_{max}, α^b,

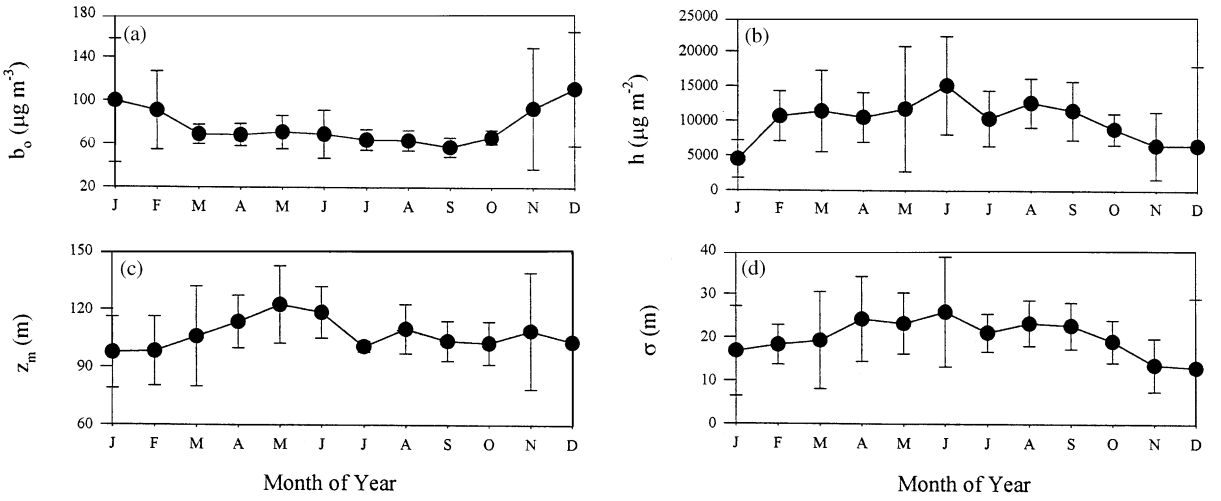


Fig. 6. Monthly means of Gaussian parameters predicted from HOT Chl profiles. Error bars represent the 95% confidence interval: (a) b_o — background Chl; (b) h — integrated Chl above b_o; (c) z_m — depth of the DCML peak; and (d) σ — standard deviation of the width of the DCML peak.

and E_k vary as a function of location and depth, it is desirable to parameterize these variables for use in the FSM.

Model simulations utilizing E_k values determined from $Chl_{[sat]}$ values yielded production rates that are consistently higher than measured values, even though adjusting E_k values to the in situ light field resulted in rates that were lower by an average of $0.24\,g\,C\,m^{-2}$ (Fig. 9a and b). The E_k values used in these simulations are maximum values and vary between stations, but are not adjusted for depth and time of day variations (Table 3). The $E_k E_{PAR}^{-1}$ parameterization method (Waters et al., 1994), which changes as a function of E_{PAR}, does vary between stations as well as with depth and time. This parameterization yielded results closer to measured values (Fig. 9c) and, consequently, was chosen as the default method for estimating E_k in the FSM (Figs. 5, 7, 10 and 11).

To calculate the average depth and time of day adjusted E_k values, surface E_k values from two diurnal experiments were combined. Surface E_k displayed a Gaussian-like pattern during the photoperiod. All E_k values measured at depth (30, 45, 75, and 100 m) during the MOBY and ACT cruises were averaged to get a representative E_k depth profile. Assuming that the diurnal variations of E_k are consistent with depth and include the maximum value during the day for each depth (i.e., 13.00 decimal hours), the E_k profile values were adjusted for diurnal variations by multiplying the values at depth z by the ratio of E_k (time of day, 0 m) to E_k (13.00 decimal hours, 0 m) to give an average time of day and depth variable E_k (Table 3). The maximum value of E_k ($442\,\mu mol\,m^{-2}\,s^{-1}$) occurred at 13.00 decimal hours at the surface while the minimum value of E_k ($25\,\mu mol\,m^{-2}\,s^{-1}$) was found at 18.58 decimal hours at 100 m. The average depth and time of day adjusted E_k model (Fig. 9d and Table 3) performed just as well as the default $E_{PAR}E_k^{-1}$ parameterization, even though there is no adjustment between HOT cruises.

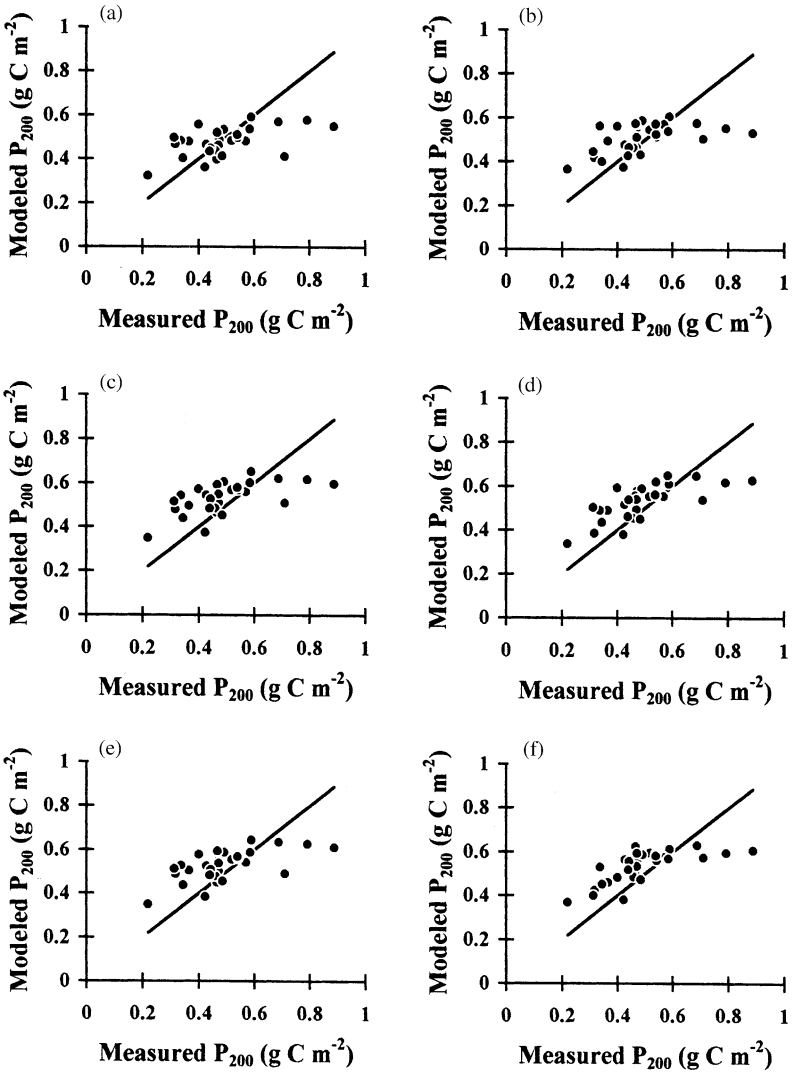


Fig. 7. Comparison of primary production predictions (HOT 23–68, 0–200 m) for different Chl reconstructions used in the full spectral model: (a) surface Chl measured from production cast held constant with depth; (b) Gaussian parameters modeled for each station from HPLC data from a different cast but the same cruise; (c) surface Chl measured for the production cast used for b_o and other Gaussian parameters used are averaged monthly binned parameters from Fig. 6; (d) Chl concentration measured for each production cast; (e) surface Chl measured for the production cast used for b_o and other Gaussian parameters used are the means determined for all cruises; and (f) average measured Chl concentration for each depth from all the production casts. A constant Φ_{max} of 0.030 mol C mol quanta^{-1}, the Bricaud et al. (1995) a_{ph} parameterization, and the $E_{par}E_k^{-1}$ parameterization of E_k were used in all model simulations. Line is $x = y$.

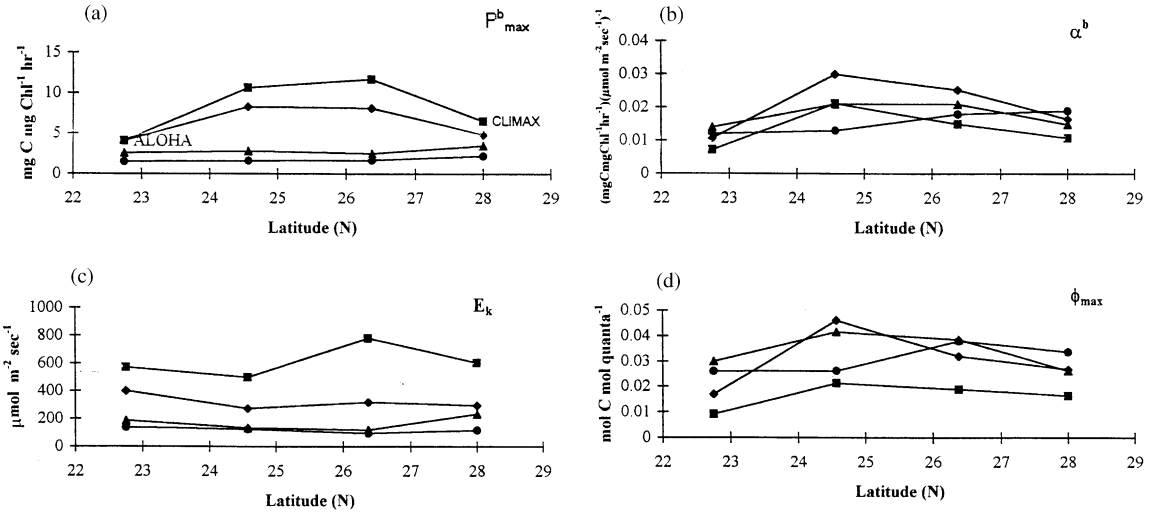


Fig. 8. Depth- and latitude-dependent variations in photosynthetic parameters estimated from P versus E measurements made during the Station ALOHA to the Climax Site transect cruise (July 1996): (a) P^b_{max} (mg C mg Chl^{-1} h^{-1}); (b) α^b ((mg C mg Chl^{-1} h^{-1}) (μmol m^{-2} s^{-1})$^{-1}$); (c) E_k (μmol m^{-2} s^{-1}); and (d) Φ_{max} (mol C mol quanta^{-1}). Results shown are from 5 m (■), 45 m (◆), 75 m (▲), and 100 m (●).

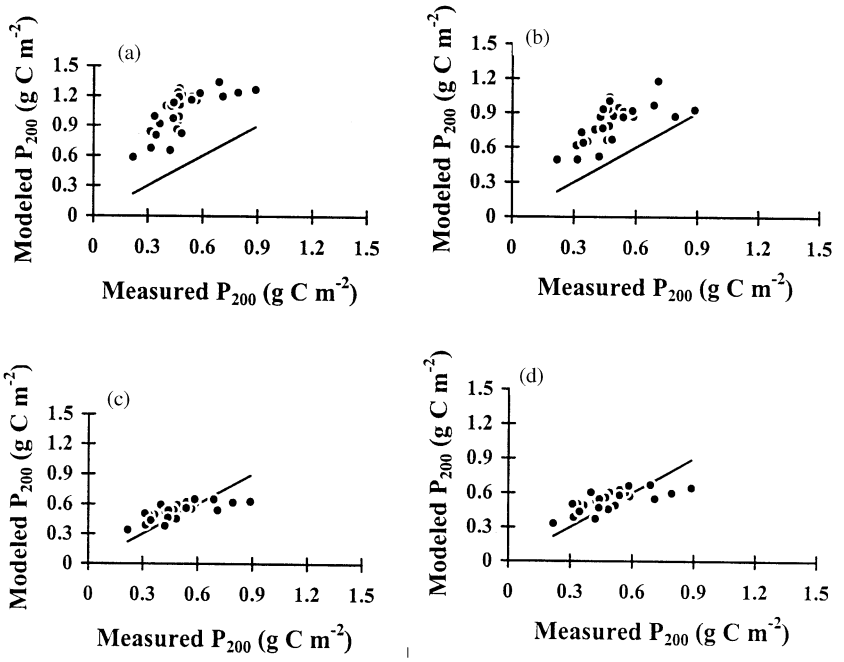


Fig. 9. Comparison of primary production predictions (HOT 23–68, 0–200 m) for different estimates of E_k used in the full spectral model: (a) constant E_k measured in photosynthetron; (b) constant E_k adjusted to in situ irradiance; (c) parameterization of $E_k E^{-1}_{par}$ from E_{par} (Waters et al., 1994); and (d) average E_k profile adjusted for diurnal variations based on data collected during the Transect and MOBY cruises (see Table 3). A constant Φ_{max} of 0.030 mol C mol quanta^{-1}, the Bricaud et al. (1995) a_{ph} parameterization, and the measured Chl profile were used in all model simulations. Line is $x = y$.

Table 3
Depth-dependent and time of day variations in E_k ($\mu mol\,m^{-2}\,s^{-1}$). Two diurnal experiments from MOBY and ACT cruises were combined to produce surface variation of E_k throughout the day which was extrapolated at depth based on measured average depth variation of E_k from all MOBY and the ACT cruises

Depth (m)	Time of day (decimal hours)							
	8.75	10.50	12.42	13.00	14.58	16.75	18.00	18.58
0	174	251	392	442	289	177	171	94
30	130	188	293	331	216	132	128	71
45	119	172	268	302	197	121	117	65
75	61	89	138	156	102	62	60	33
100	52	76	118	133	86	53	51	28
200	20	28	44	50	32	20	19	10

3.3. Phytoplankton absorption and quantum yield

All of the a_{ph} parameterizations tested yielded mean production rates that are similar to those measured at Station ALOHA (Fig. 10). The Bricaud et al. (1995) open-water parameterization yielded a mean daily primary production rate of $0.528\,g\,C\,m^{-2}$, a value that most closely resembled the mean measured rate of $0.510\,g\,C\,m^{-2}$ (Fig. 10a). The a_{ph} model utilizing Morel's (1988) 14 species average spectrum produced estimates lower than those measured (Fig. 10c and Table 2). When the spectral reconstruction (Fig. 10b) and Kishino (Fig. 10e) methods were utilized, the mean modeled daily primary production rates were 9 and 6% higher, respectively, than those measured.

When a_{cdom} was omitted from the water-column absorption calculations (Fig. 10d), there was a 20% increase in modeled production rates. Detrital absorption determined by the Kishino et al. (1985) method was $< 10\%$ of a_{ph}, which increased mean daily production rates by 10% when this absorption term is included in the FSM (Fig. 10f).

Photosynthesis rate is linearly related to Φ_{max} (Eqs. (1) and (2)). As a consequence, all simulations utilizing constant Φ_{max} values yielded a correlation coefficient of 0.713 (Table 2). Model predictions based on the default value of $0.03\,mol\,C\,mol\,quanta^{-1}$ are shown in Figs. 5 and 7d. The average Φ_{max} (± 1 SD) of all experiments from the ACT and MOBY cruises combined was $0.026 \pm 0.009\,mol\,C\,mol\,quanta^{-1}$ ($n = 48$). The average Φ_{max} value for two "diatom" stations encountered during the ACT cruise was $0.033\,mol\,C\,mol\,quanta^{-1}$ ($n = 8$) and the overall average Φ_{max} value for all samples minus the diatom stations was $0.024\,mol\,C\,mol\,quanta^{-1}$ ($n = 40$). The effect of utilizing different Φ_{max} values was tested in the full spectral model (see Table 2).

Two attempts were made to vary Φ_{max} between HOT cruises. Φ_{max} for each cruise was calculated from a_{ph} and α (for photosynthetron irradiance) that were each parameterized as a function of $Chl_{[sat]}$ using Chl regression relationships determined at all depths from the ACT and MOBY cruises (Table 1). When Φ_{max} measured during the ACT and MOBY cruises was directly regressed against Chl, Chl explained 67% of the Φ_{max} variability (Table 1). Integrated primary production

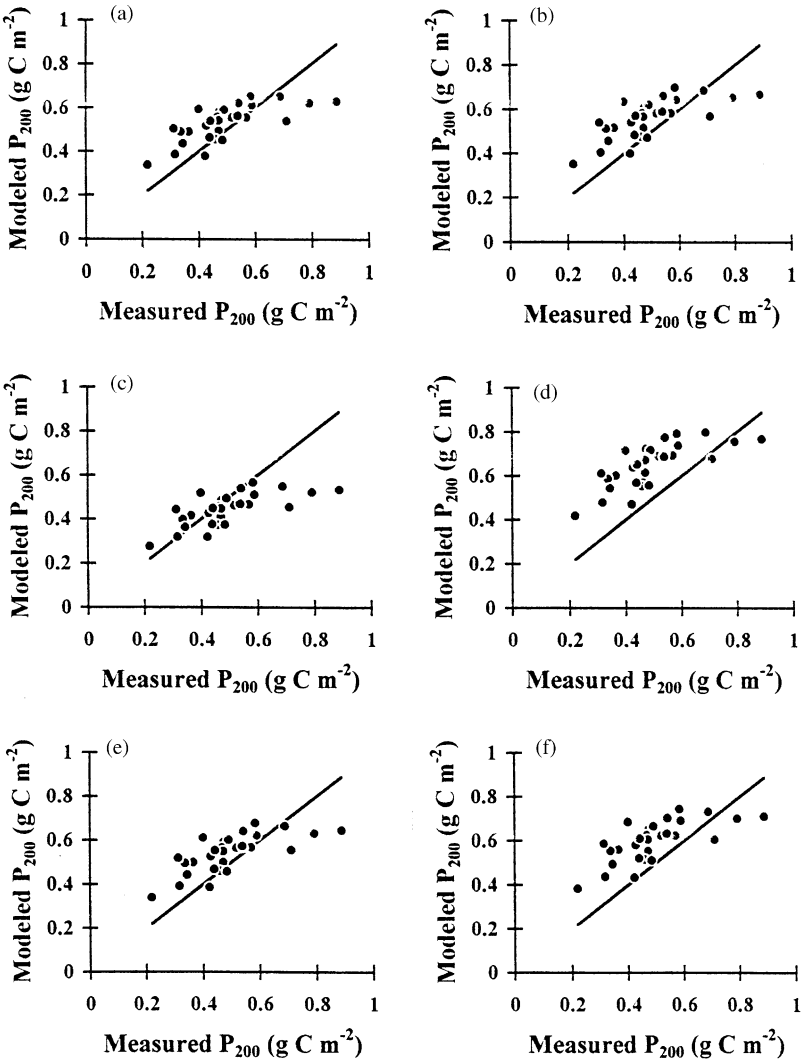


Fig. 10. Comparison of primary production predictions (HOT 23–68, 0–200 m) for different estimates of phytoplankton absorption used in the full spectral model: (a) Bricaud et al. (1995) a_{ph} parameterization; (b) average a_{ph} (Fig. 2) from the ACT cruise determined via the spectral reconstruction method; (c) Morel (1988) a_{ph} parameterization; (d) Bricaud et al. (1995) a_{ph} parameterization with a_{cdom} omitted in light attenuation calculations; (e) average a_{ph} (Fig. 2) from the Transect cruise determined with the filter pad technique; and (f) average a_p from the ACT cruise determined from the filter-pad technique (including detrital absorption). A constant Φ_{max} of 0.030 mol C mol quanta^{-1}, the measured Chl profile, and the E_{par}/E_k parameterization of E_k were used in all model simulations. Line is $x = y$.

estimates (0–200 m) using Φ_{max} determined from $Chl_{[sat]}$ regressions, indirectly and directly, did not agree with the measured rates (Table 2).

The "average" Φ_{max} method described above utilizes a constant Φ_{max} between stations, and between depth and time of day. The Φ_{max} values determined from $Chl_{[sat]}$ regressions vary between

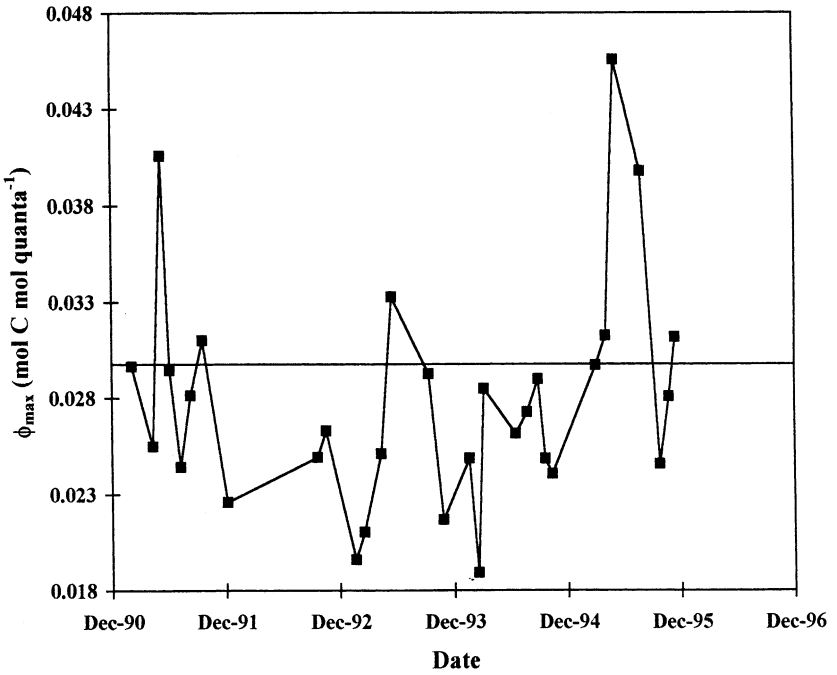


Fig. 11. Cruise-specific variations in Φ_{max} calculated by setting the FSM to equal measured production and solving for Φ_{max}. The solid line represents the Φ_{max} default value of 0.03 mol C mol quanta^{-1}.

stations but not depth or time of day. In an effort to vary Φ_{max} with depth and time of day, Φ_{max} values from the two diurnal experiments were combined; all the values of Φ_{max} measured at depth (30, 45, 75, and 100 m) during the MOBY and ACT cruises were averaged to get a representative Φ_{max} depth profile throughout the day. Model results utilizing the average depth and time of day Φ_{max} values yielded daily integrated production rates that were 39% higher than those measured at Station ALOHA (data not shown).

4. Discussion

Short-term P versus E measurements are thought to provide an estimate of gross photoautotrophic production, while the "standard" ^{14}C productivity determination performed during the photoperiod corresponds to net photoautotrophic production minus any heterotrophic respiratory losses (Platt et al., 1989; Karl et al., 1998). The fact that the FSM predictions are similar to the in situ primary productivity rates (Fig. 5 and Table 4) suggests that respiratory losses during the photoperiod are equivalent (percentage basis) to those occurring over short intervals during the photoperiod. Evidence to support the latter has recently been published by Karl et al. (1998), who found that the rates of primary productivity and DO^{14}C production are linearly correlated at Station ALOHA. Alternatively, it is possible that the good agreement between the modeled and measured rates is fortuitous because of uncertainties in model assumptions (e.g., the constant

Table 4
Mean annual phytoplankton primary production rates ($g\,C\,m^{-2}$) estimated for the North Pacific Subtropical Gyre

Method	Time interval	Rate ± SD
Measured[a]	1991–1995	181 ± 18
FSM[b]	1991–1995	168 ± 12
B & F[c]	1978–1983	74
A & M[d]	1978–1983	91
L[e]	1978–1983	59

[a] ^{14}C method, 12 h in situ incubation (Karl and Lukas, 1996).
[b] Full spectral model $\Phi_{max} = 0.026\,mol\,C\,mol\,quanta^{-1}$ and reconstructed Chl(z).
[c] CZCS $Chl_{[sat]}$ (Fig. 9 in Behrenfeld and Falkowski, 1997).
[d] CZCS $Chl_{[sat]}$ (Table 2 in Antoine and Morel, 1996).
[e] CZCS $Chl_{[sat]}$ (Table 1 in Longhurst et al., 1995).

Φ_{max} term) and/or the ^{14}C method itself. Unfortunately, the present data set does not allow us to distinguish between these (or alternative) explanations.

4.1. *Effect of Chl profiles on* $P_{200\,m}$

The different Chl profile parameterizations utilized to calculate $P_{200\,m}$ in Fig. 7 allow us to draw three conclusions concerning the limitations of only measuring Chl in the top attenuation length of the water column. First, when $Chl_{[sat]}$ is assumed to be constant with depth, the FSM yields lower estimates of production and a lower correlation with measured production (Table 2). Production above background levels in the DCML (defined as $P_{200\,m}$ modeled utilizing measured Chl concentrations minus $P_{200\,m}$ estimates modeled utilizing constant surface Chl concentrations at depth) is responsible for an average of 8.4% of $P_{200\,m}$ during 1991–1995. Second, simply accounting for the average production above background levels in the DCML improves model performance (Fig. 7a versus 7b–f). Results from the FSM using Gaussian parameters from a different cast but the same cruise (Fig. 7b) did not improve the model results over those obtained with monthly averaged parameters (Fig. 7c). In fact, Letelier et al. (1996) have shown that intracruise variability in Chl profiles is just as large as between cruise variations. Third, knowledge of surface Chl is more important than knowledge of Chl(z). The mean value of daily $P_{200\,m}$ utilizing $Chl_{[sat]}$ and monthly averaged Gaussian profile parameters ($0.536 \pm 0.070\,g\,C\,m^{-2}$) is not significantly different (t-test, $P > 0.69$) from the daily $P_{200\,m}$ mean value of $0.528 \pm 0.080\,g\,C\,m^{-2}$ computed using the measured Chl profile. However, the daily $P_{200\,m}$ values computed utilizing Gaussian parameters, estimated from the HPLC cast performed during the same cruise were lower on average ($0.507\,g\,C\,m^{-2}$).

Intracruise variability in Chl profiles is caused, in part, by internal waves that vertically displace isopycnals (Letelier et al., 1996). To analyze the sensitivity of our production estimates to the sampling bias resulting from intracruise fluctuations in the DCML, Chl concentrations were related to density values for HOT 23 (February 1991). Density values from seven repetitive casts were used to assign Chl concentrations with depth and FSM production estimates were rerun

for HOT 23 using the new set of Chl profiles. During the 8 h sampling period, the 1024.00 kg m^{-3} "mixed-layer" isopycnal varied from 10 to 73 m and the 1024.24 kg m^{-3} "DCML" isopycnal varied from 89 to 128 m. Despite the variations in Chl(z), $P_{200\,m}$ values varied by only 4% from the lowest value when the DCML peak was at 128 m from the highest value when the DCML peak was at 89 m. The results of this model simulation are expected because the background Chl concentrations are responsible for an average of 92% of $P_{200\,m}$ from 1991 to 1995. However, this simulation may be underestimating the influence of vertical oscillations on production if the fluctuations are injecting nutrients into the mixed layer (McGowan and Hayward, 1978) or preferentially stimulating specific phytoplankton populations (Venrick, 1993).

4.2. Measured versus modeled production rates

A frequent pattern observed in our depth-integrated production rate comparisons was that the slope between the modeled and measured results was consistently less than unity (Figs. 7, 9 and 10; Table 2). This results in low-productivity casts having higher modeled productivity, and high-productivity casts being underestimated. These errors are not associated with predicting Chl(z) because the model results using measured Chl profiles display the same pattern (Fig. 7c and d). The error therefore must result from our estimations of Φ_{max} and a_{ph}. Both of these parameters vary with light history and nutrient availability (Cleveland et al., 1989; Marra and Bidigare, 1994; Ondrusek and Bidigare, 1997), which in turn can influence phytoplankton community composition. Pigments in surface waters of the NPSG are not very diverse and have signatures characteristic of small prokaryotic photoautotrophs (Ondrusek et al., 1991; Letelier et al., 1993; Andersen et al., 1996). It is hypothesized that on high-production days at Station ALOHA (measured production >0.6 g C m^{-2}), where our model tends to underestimate production (Figs. 7 and 9–11), there is an associated population shift to other dominant groups such as diatoms (Scharek et al., 1998; Venrick, 1993) or *Trichodesmium* (Karl et al., 1996). This will subsequently alter phytoplankton absorption properties, especially with regard to the fraction of absorbed light that is used for photosynthesis. A higher fraction of light absorbed by non-photosynthetically active pigments will decrease Φ_c (Bidigare et al., 1987, 1989). Our model does not distinguish between photosynthetic and non-photosynthetic pigments and does not vary Φ_{max} between cruises.

Careful determination and parameterization of Φ_{max} is essential. Lowering Φ_{max} by 0.001 mol C (mol quanta)$^{-1}$, decreased mean daily production estimates at Station ALOHA for 1991–1995 by 0.018 g C m^{-2}. The variation in Φ_{max} responsible for the bias in our high and low estimates of $P_{200\,m}$ can be estimated by setting the FSM to equal measured production and solving for Φ_{max}. The cruise-specific values of Φ_{max} range from 0.019 to 0.046 mol C (mol quanta)$^{-1}$, with a mean value of 0.028 ± 0.006 mol C (mol quanta)$^{-1}$ (Fig. 11; Table 2). More work is required in predicting time-dependent values of Φ_{max}.

Measured and modeled ($\Phi_{max} = 0.026$ mol C (quanta)$^{-1}$, Chl$_{[sat]}$ and monthly averaged Gaussian-described Chl profiles) $P_{200\,m}$ values were plotted over time to identify anomalous periods where the modeled values deviate from measured values (Fig. 12). The modeling results are encouraging since the inflections in the measured data are highly correlated to the model simulations. The highest production rates (>0.7 g C m^{-2}) occurred during May 1991, February and June 1992, May 1993, and May 1995. All of the these high-production periods occurred in late

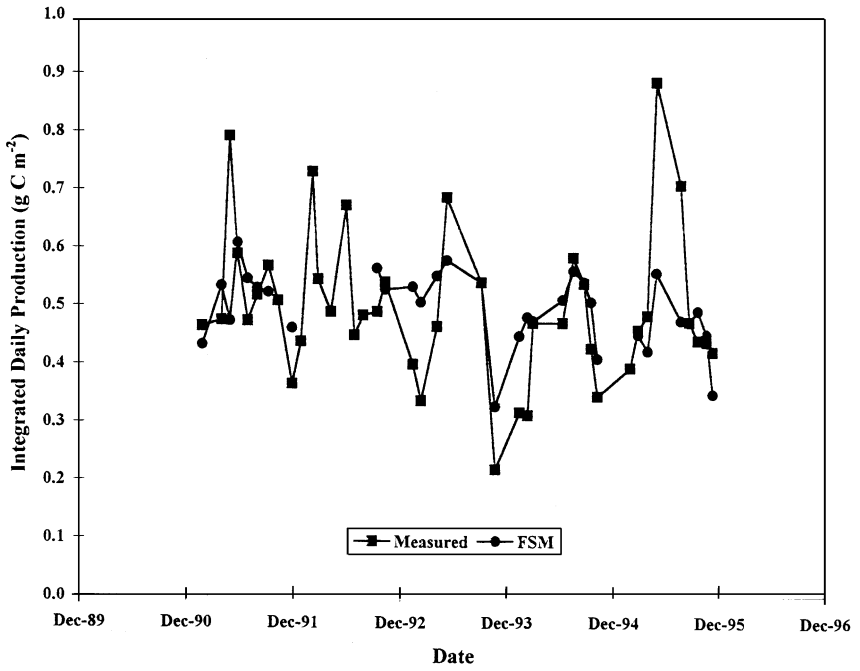


Fig. 12. Variation in measured (■) and modeled (●) primary production over time (HOT 23–68). Full spectral model predictions were calculated using a Φ_{max} value of 0.026 mol C (mol quanta)$^{-1}$, surface Chl measured from the production cast for b_o, and averaged monthly Gaussian parameters to reconstruct the Chl profiles.

spring and early summer, and all had near-average surface Chl values. The only Gaussian profile parameter that showed anomalous behavior during these periods was z_m, which had high values, indicating that the DCML was deeper than average. Fucoxanthin was at the high end of its annual range (about 18 ng l^{-1} located above the DCML), implying that an increase in the local diatom population may have been partly responsible for the increase in production during these periods. During the high-production periods, surface temperatures were increasing from the winter low of $\sim$23°C and the mixed-layer depth was starting to shoal. The combination of nutrient injections from winter mixing and the onset of stratification appears to be an important factor in regulating primary production rates at Station ALOHA. If these events can be detected via satellite imagery (e.g., TOPEX/Poseidon), Φ_{max} values could be adjusted accordingly for use in the FSM.

4.3. Comparison to other models

We compared our regional model to the global P^b_{opt} production model of Behrenfeld and Falkowski (1997). Their annual global estimate of primary production of 43.5 Pg C yr^{-1} compares well with other estimates of global production utilizing absorption-based (Antoine et al., 1996) and photosynthesis-irradiance-based (Longhurst et al., 1995) models (see Table 2 in Behrenfeld and Falkowski, 1997). According to their global map of mean annual production using CZCS data (1978–1983), estimates of primary production for the NPSG are ca. two-fold lower than our model

estimates for Station ALOHA. Their average annual production rate of $\sim 74\,g\,C\,m^{-2}$ was significantly lower than the FSM estimate of $168 \pm 12\,g\,C\,m^{-2}$ and the mean measured value of $181 \pm 18\,g\,C\,m^{-2}$ (Table 4). Falkowski and Wilson (1992) calculated an average annual production rate, based on a square-root function of surface Chl concentration, of $189 \pm 85\,g\,C\,m^{-2}$ for the North Pacific Ocean; however, this estimate included the equatorial and subarctic Pacific regions in addition to the NPSG. These disparities were explored by applying the input data described herein to the equations given in Behrenfeld and Falkowski (1997). Annual production estimates for 1991–1995 utilizing the Behrenfeld and Falkowski (1997) model with measured Chl concentrations averaged $100 \pm 5\,g\,C\,m^{-2}$. Substituting both measured Chl and P^b_{opt} values determined at Station ALOHA (1991–1995) increased the average annual estimate to $154 \pm 24\,g\,C\,m^{-2}$, a value that is slightly lower than the measured and FSM-modeled rates.

It is reasonable to expect the production estimate at one location to be off by a factor of two due to the generalizations required to describe a range of dynamic oceanic environments. Behrenfeld and Falkowski (1997) estimate P^b_{opt} as a polynomial function of temperature where values increase with temperature up to 20°C then decrease as temperature increases from 20 to 29°C. Behrenfeld and Falkowski's (1997) temperature-dependent parameterization of P^b_{opt} produced a mean daily P^b_{opt} value for Station ALOHA (1991–1995) of $55 \pm 5\,g\,C\,g\,Chl^{-1}$, which is 1.5-fold lower and less variable than the measured daily P^b_{opt} values ($84 \pm 30\,g\,C\,g\,Chl^{-1}$; Fig. 13). This, in part,

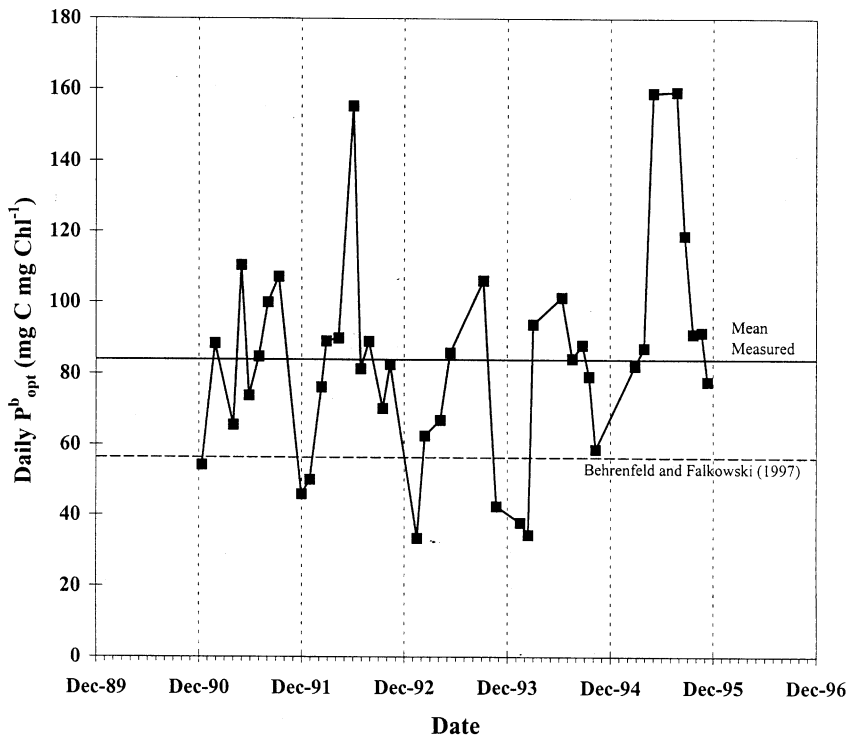


Fig. 13. Maximum in situ Chl-specific primary production (P^b_{opt}) measured at Station ALOHA during 1991–1995. The solid and dashed lines correspond to the mean measured and modeled (Behrenfeld and Falkowski, 1997) daily P^b_{opt} values during this period.

contributed to the low P^{b}_{opt}-based estimates when modeling NPSG data during 1991–1995. The remaining offset is attributable to differences in the depth of integration (100 m for the P^{b}_{opt} model and 200 m for the FSM).

Antoine et al. (1996) estimated global production estimates utilizing an absorption-based model similar to the FSM utilized in this study; yet their production rate estimates for the NPSG (1978–1983) are one-half of those measured at Station ALOHA during 1991–1995. Their global primary production estimates, however, are similar to Behrenfeld and Falkowski (1997). They parameterized Φ_{max} based on P^{b}_{max} values estimated using the exponential temperature-dependent model of Eppley (1972), with P^{b}_{max} values normalized to 4.6 g C g Chl^{-1} h^{-1} at 20°C. Using this parameterization, P^{b}_{max} values averaged 6.3 g C g Chl^{-1} h^{-1} for Station ALOHA during 1991–1995. This P^{b}_{max} value is close to the average of 6.6 g C g Chl^{-1} h^{-1} measured in this study. Antoine et al. (1996) estimate water column production utilizing a series of look-up tables based on phytoplankton physiological parameters. Their lower estimates of integrated production for the NPSG result from other structures in their model.

P^{b}_{max} parameterization in Longhurst et al. (1995) is based on extrapolating region-specific values based on environmental conditions and data collected in the North Atlantic Ocean. The Longhurst et al. (1995) production results are similar to Behrenfeld and Falkowski (1997) and Antoine et al. (1996) during 1978–1983 in the NPSG. Longhurst et al. (1995) utilize a P^{b}_{max} value for the North Pacific Subtropical Gyre of 3.4 g C g Chl^{-1} h^{-1}. This value is much lower than the mean P^{b}_{max} value of 6.6 g C g Chl^{-1} h^{-1} reported at Station ALOHA and contributes to the low primary production estimates predicted for the NPSG.

The Chl-specific maximum production rates predicted regulate the magnitude of the depth-integrated production estimates of all the models discussed above. All three models utilized the same CZCS Chl data set in their global production estimates. However, the Chl-specific maximum production rates used in the Longhurst et al. (1995) and Behrenfeld and Falkowski (1997) models are lower than that used in the Antoine et al. (1996) model and those measured at Station ALOHA (1991–1995). The lower parameterized estimates of P^{b}_{opt} and P^{b}_{max} may be, at least in part, artifacts of low historical estimates of oligotrophic primary production rates resulting from trace metal-contaminated data sets. Conversely, they may represent decadal-scale variations in photophysiology. Primary production estimates made at Station ALOHA since 1989 have been consistently higher than historical estimates (Karl and Lukas, 1996; Karl et al., 2001), indicating that the maximum production rates in the NPSG have increased over the last several decades.

The measured rate of annual production at Station ALOHA (181 g C m^{-2}) can be compared to other study sites by calculating Ψ^*, the cross section for photosynthesis per unit Chl (m^2 g Chl^{-1}; Morel, 1991). Assuming an integrated Chl level of 0.02 g m^{-2} (Fig. 4) and yearly radiation of 3×10^9 J m^{-2} (ISCCP data) for Station ALOHA, one obtains a Ψ^* value of 0.12 m^2 g Chl^{-1}. While this value is 1.7-fold higher than historical values (0.07 g Chl^{-1}; Morel, 1978), it is nearly identical to that determined for the Bermuda Atlantic Time-series Study (BATS) site (Siegel et al., 2001). We conclude, therefore, that the "high" contemporary rates of primary production observed for Station ALOHA are real and similar to those reported for the Sargasso Sea.

Based upon the recalculation of euphotic zone primary production estimates using the Behrenfeld and Falkowski (1997) model, the difference in Chl concentration between the 1978–1983 CZCS data and 1991–1995 HPLC data is responsible for $\sim 25\%$ of the difference in model estimates.

Table 5
Seasonal variations in surface Chl concentrations at Station ALOHA ($\mu g l^{-1} \pm 1SD$). Winter is defined as January–March, spring is defined as April–June, summer is defined as July–September, and fall is defined as October–December

Method	Year	Winter	Spring	Summer	Fall
HPLC[a]	1991–1995	0.07 ± 0.01	0.06 ± 0.01	0.08 ± 0.02	0.09 ± 0.03
FL[a]	1991–1995	0.08 ± 0.01	0.07 ± 0.02	0.09 ± 0.02	0.09 ± 0.03
CZCS[b]	1978–1986	0.05 ± 0.01	0.05 ± 0.01	0.06 ± 0.02	0.06 ± 0.01
SeaWiFS[b]	1997–1998	0.08 ± 0.01	0.10 ± 0.02	0.09 ± 0.01	0.10 ± 0.01

[a]Average for upper 10 m from bottle cast data.
[b]Average concentration for a 20–24°N, 156–160°W box about Station ALOHA.

Seasonally averaged CZCS Chl data were significantly lower (t-test, $P < 0.05$) than those measured at Station ALOHA by HPLC in the fall and winter months (Table 5). For all seasons, the CZCS Chl data from 1978 to 1983 were $\sim 25\%$ lower than the HPLC-determined Chl concentration. Inconsistent Chl measurement techniques and climatic events on dissimilar time scales can potentially obscure long-term Chl trends. Venrick et al. (1987) compiled 17 yr of Chl data collected from 1968 to 1985 at the CLIMAX site (128°N, 155°W). Samples were collected using GF/C filters and analyzed fluorometrically. There was a significant interannual trend of increasing integrated Chl over time; however, most of the increase occurred in the DCML with no statistical increase in the mixed-layer concentrations (Venrick, 1993). These patterns were confirmed by Karl et al. (2001) who analyzed three decades of Chl data collected at Stations CLIMAX and ALOHA. CZCS Chl data for 1978–1986 averaged $0.06 \pm 0.01\,mg\,m^{-3}$ in the vicinity of Station ALOHA (Table 5) while the HPLC data for 1991–1995 averaged $0.08 \pm 0.01\,mg\,m^{-3}$. CZCS Chl data are being reprocessed and concentration estimates are expected to increase because of algorithm improvements (Myrmehl and Morel, 1994). Nevertheless, historical Chl concentrations only account for 25% of the difference in model estimates of primary production for Station ALOHA.

It is clear that the CZCS-based productivity estimates in Table 4 are lower than those measured at Station ALOHA during 1991–1995. This is a result of utilizing different Chl concentrations, Chl-specific maximum production rates, and other model parameterizations. Whether or not the differences in Chl concentration and P^b_{opt} are real or artifactual, the parameterizations utilized in historical models for the NPSG must be revised. One of the goals of the SeaWiFS project is to provide accurate global primary production estimates. By applying the Behrenfeld and Falkowski (1977) model to the HOT data set, it can be seen that knowledge of local P^b_{opt} and Chl values can greatly improve model predictions; it also demonstrates the need for continuous local investigations to update our understanding of the processes that regulate model input parameters. Regional investigations such as this study and the HOT program are required for accurate global carbon uptake estimates in a constantly evolving ecosystem. By updating the parameters used by Behrenfeld and Falkowski (1997) and assuming that the rates are consistent for all oligotrophic waters in the World's Ocean, the estimate of annual global production is increased by $\sim 25\%$ from 43 to 54 Pg C.

5. Conclusions

The complexities in the absorption-based model described herein demonstrate why the use of simple empirical models is so popular when estimating production rates from remotely sensed data. The goal of this investigation was to understand the controls on phytoplankton production rates and at the same time improve our ability to predict primary production rates from remote sensing platforms. At present, with just $Chl_{[sat]}$ and daily E_{PAR} measurements, the FSM can account for $\sim$50% of the variability in measured production rates in the NPSG. By comparison, this model only accounted for 35% of the variability of measured production rates at the BATS site (-16% bias, Gaussian-reconstructed Chl(z), $n = 82$; D.A. Siegel, pers. comm.). Differences in model performance at these two US JGOFS time-series sites probably result from the higher degree of variability of Φ_{max} at the BATS site relative to the HOT site (Ondrusek and Bidigare, 1997; Sorensen and Siegel, 2001). Analysis of model limitations can provide insight into the processes that need to be addressed to improve model performance. Periods of high production rates that are not manifested in increased $Chl_{[sat]}$ concentrations will continue to limit our primary production predictive capabilities.

Future work must include investigations on how variations in Φ_{max} can be detected via satellites. For example, Φ_{max} may be parameterized using relationships developed with sea-surface altimeter data. This will likely involve monitoring this and other remotely sensed variables (e.g., temperature, wind speed, and solar insulation). In the NPSG, understanding phytoplankton community shifts from small prokaryote-dominated systems to large eukaryote-dominated systems appears to be one of the key elements to improving FSM performance. Despite the limitations of the model described here, the FSM was able to predict primary production rates from available remotely sensed data that are not significantly different from measured values. It is emphasized that this level of quality in model performance is not possible without constant monitoring of the local environments through programs such as HOT at Station ALOHA.

Acknowledgements

This research was supported by NASA grants NAGW-3439 and NAG5-7171 (RRB), NOAA grant NA37RJ0199 (RRB) and NSF grants OCE-9301368 (DMK) and OCE96-17409 (DMK and RRB), OCE-9303094 (R. Lukas) and OCE-9315311 (RRB), SOEST contribution #5303 and US JGOFS #627. This project would not have been possible without the collaborative efforts of the US JGOFS HOT and the NOAA/NASA MOBY (D. Clark) programs and the numerous personnel whose combined expertise and dedication are unrivaled. We wish to acknowledge Dr. B. Prézelin and A. Matlick for their help in designing the photosynthetrons and we also wish to thank C. Trees and M. Behrenfeld for helpful comments on the manuscript.

References

Andersen, R.A., Bidigare, R.R., Keller, M.D., Latasa, M., 1996. A comparison of HPLC pigment signatures and electron microscopic observations for oligotrophic waters of the North Atlantic and Pacific Oceans. Deep-Sea Research 43, 517–538.

Antoine, D., Andre, J., Morel, A., 1996. Oceanic primary production 2. Estimation at global scale from satellite (Coastal Zone Color Scanner) chlorophyll. Global Biogeochemical Cycles 10, 57–69.

Behrenfeld, J.M., Falkowski, P.G., 1997. Photosynthetic rates derived from satellite-based chlorophyll concentration. Limnology and Oceanography 42, 1–20.

Bidigare, R.R., Ondrusek, M.E., 1996. Spatial and temporal variability of phytoplankton pigment distributions in the central equatorial Pacific Ocean. Deep-Sea Research II 43, 809–833.

Bidigare, R.R., Ondrusek, M.E., Morrow, J.H., Kiefer, D.A., 1990. In vivo absorption properties of algal pigments. Society of Photo-Optical Instrumentation Engineers 1302, 290–302.

Bidigare, R.R., Prézelin, B.B., Smith, R.C., 1992. Bio-optical models and the problems of scaling. In: Falkowski, P.G., Woodhead, A.D. (Eds.), Primary Productivity and Biogeochemical Cycles in the Sea. Plenum Press, New York, pp. 175–212.

Bidigare, R.R., Schofield, O., Prézelin, B.B., 1989. Influence of zeaxanthin on quantum yield of photosynthesis of *Synechococcus* clone WH7803 (DC2). Marine Ecology Progress Series 56, 177–178.

Bidigare, R.R., Smith, R.C., Baker, K.S., Marra, J., 1987. Oceanic primary production estimates from measurements of spectral irradiance and pigment concentrations. Global Biogeochemical Cycles 1, 171–186.

Bishop, J.K.B., Rossow, W.B., Dutton, E.G., 1997. Surface solar irradiance from the International Satellite Cloud Climatology Project 1983–1991. Journal of Geophysical Research 102, 6883–6910.

Bricaud, A., Babin, M., Morel, A., Claustre, H., 1995. Variability in the chlorophyll-specific absorption coefficients of natural phytoplankton: analysis and parameterization. Journal of Geophysical Research 100, 13321–13332.

Cleveland, J.S., Perry, M.J., Kiefer, D.A., Talbot, M.C., 1989. Maximal yield of photosynthesis in the northwestern Sargasso Sea. Journal of Marine Research 47, 869–886.

Cullen, J.J., Lewis, M.R., Davis, C.O., Barber, R.T., 1992. Photosynthetic characteristics and estimated growth rates indicate grazing is the proximate control of primary production in the equatorial Pacific. Journal of Geophysical Research 97, 639–654.

Eppley, R.W., 1972. Temperature and phytoplankton growth in the sea. Fisheries Bulletin 70, 1063–1084.

Falkowski, P.G., Wilson, C., 1992. Phytoplankton productivity in the North Pacific Ocean since 1900 and implications for absorption of anthropogenic CO_2. Nature 358, 741–743.

Fitzwater, S.E., Knauer, G.A., Martin, J.H., 1982. Metal contamination and its effect on primary production measurements. Limnology and Oceanography 27, 544–551.

Goericke, R., Repeta, D.J., 1993. Chlorophylls *a* and *b* and divinyl chlorophylls *a* and *b* in the open subtropical North Atlantic Ocean. Marine Ecology Progress Series 101, 307–313.

Hooker, S.B., Esaias, W.E., Feldman, G.C., Gregg, W.W., McClain, C.R. 1992. An overview of SeaWiFS and ocean color. NASA Technical Memorandum 104566, Vol. 1, 24pp.

Jassby, A.T., Platt, T., 1976. Mathematical formulation of the relationship between photosynthesis and light for phytoplankton. Limnology and Oceanography 21, 540–547.

Karl, D.M., Bidigare, R.R., Letelier, R.M., 2001. Long-term changes in plankton community structure and productivity in the North Pacific Subtropical Gyre: The domain shift hypothesis. Deep-Sea Research II 48, 1449–1470.

Karl, D.M., Christian, J.R., Dore, J.E., Hebel, D.V., Letelier, R.M., Tupas, L.M., Winn, C.D., 1996. Seasonal and interannual variability in primary production and particle flux at Station ALOHA. Deep-Sea Research II 43, 539–568.

Karl, D.M., Hebel, D.V., Bjorkman, K., Letelier, R.M., 1998. The role of dissolved organic matter release in the productivity of the oligotrophic North Pacific Ocean. Limnology and Oceanography 43, 1270–1286.

Karl, D.M., Lukas, R., 1996. The Hawaii Ocean Time-series (HOT) program: background, rationale and field implementation. Deep-Sea Research II 43, 129–156.

Kishino, M., Takahashi, M., Okama, N., Ichimura, S., 1985. Estimation of the spectral absorption coefficients of phytoplankton in the sea. Bulletin of Marine Science 37, 634–642.

Letelier, R.M., Bidigare, R.R., Hebel, D.V., Ondrusek, M., Winn, C.D., Karl, D.M., 1993. Temporal variability of phytoplankton community structure based on pigment analysis. Limnology and Oceanography 38, 1420–1437.

Letelier, R.M., Dore, J.E., Winn, C.D., Karl, D.M., 1996. Seasonal and interannual variations in photosynthetic carbon assimilation at Station ALOHA. Deep-Sea Research II 43, 467–490.

Lewis, M.R., Cullen, J.J., Platt, T., 1983. Phytoplankton and thermal structure in the upper ocean: consequences of nonuniformity in chlorophyll profile. Journal of Geophysical Research 88, 2565–2570.

Lewis, M.R., Smith, J.C., 1983. A small volume, short-incubation-time method for measurement of photosynthesis as a function of incident irradiance. Marine Ecology Progress Series 13, 794–806.

Lindley, S.T., Bidigare, R.R., Barber, R.T., 1995. Phytoplankton photosynthesis parameters along 140°W in the equatorial Pacific. Deep-Sea Research II 42, 441–463.

Longhurst, A., Sathyendranath, S., Platt, T., Caverhill, C., 1995. An estimate of global primary production in the ocean from satellite radiometer data. Journal of Plankton Research 17, 1245–1271.

Marra, J., Bidigare, R.R., 1994. The question of a nutrient effect on the bio-optical properties of phytoplankton. Society of Photo-Optical Instrumentation Engineers 2258, 152–162.

McGowan, J.A., Hayward, T.L., 1978. Mixing and oceanic productivity. Deep-Sea Research 25, 771–793.

Morel, A., 1978. Available, usable, and stored radiant energy in relation to marine photosynthesis. Deep-Sea Research 25, 673–688.

Morel, A., 1988. Optical modeling of the upper ocean in relation to its biogenous matter content (Case 1 Waters). Journal of Geophysical Research 93, 10 749–10 768.

Morel, A., 1991. Light and marine photosynthesis: a spectral model with geochemical and climatological implications. Limnology and Oceanography 26, 263–306.

Myrmehl, C., Morel, A., 1994. Accounting for the marine reflectance bidirectionality when processing remotely sensed ocean colour data. Society of Photo-Optical Instrumentation Engineers 2258, 870–878.

Neale, P., Richerson, P.J., 1987. Photoinhibition and the diurnal variation of phytoplankton photosynthesis — I. Development of a photosynthesis–irradiance model from studies of in situ responses. Journal of Plankton Research 19, 167–193.

Ondrusek, M.E., Bidigare, R.R., 1997. Measurements of photo-physiological parameters and primary production in the Central North Pacific Ocean. Society of Photo-Optical Instrumentation Engineers 2963, 874–879.

Ondrusek, M.E., Bidigare, R.R., Sweet, S.T., Defreitas, D.A., Brooks, J.M., 1991. Distribution of phytoplankton pigments in the North Pacific Ocean in relation to physical and optical variability. Deep-Sea Research 38, 243–266.

Platt, T., Harrison, W.G., Lewis, M.R., Li, W.K.W., Sathyendranath, S., Smith, R.E., Vezina, A.F., 1989. Biological production of the oceans: the case for a consensus. Marine Ecology Progress Series 52, 77–88.

Platt, T., Sathyendranath, S., Caverhill, C.M., Lewis, M.R., 1988. Ocean primary production and available light: further algorithms for remote sensing. Deep-Sea Research 35, 855–879.

Prézelin, B.B., Bidigare, R.R., Matlick, H.A., Putt, M., Hoven, B.V., 1987. Diurnal patterns of size-fractioned primary productivity across a coastal front. Marine Biology 96, 563–574.

Prieur, L., Sathyendranath, S., 1981. An optical classification of coastal and oceanic waters based on the specific spectral absorption curves of phytoplankton pigments, dissolved organic matter, and other particulate materials. Limnology and Oceanography 26, 671–689.

Scharek, R., Latasa, M., Karl, D.M., Bidigare, R., 1998. Temporal variations in diatom abundance and downward vertical flux in the oligotrophic North Pacific gyre. Deep-Sea Research 46, 1051–1075.

Schofield, O., Bidigare, R.R., Prézelin, B.B., 1990. Chromatic photoadaptation and enhancement effects on wavelength-dependent quantum yield and productivity in the diatom *Chaetoceros gracile* and the prymnesiophyte *Emiliania huxleyi*. Marine Ecology Progress Series 64, 168–175.

Schofield, O., Prezelin, B.B., Bidigare, R.R., Smith, R.C., 1993. In situ photosynthetic quantum yield. Correspondence to hydrographic and optical variability within the Southern California Bight. Marine Ecology Progress Series 64, 25–37.

Siegel, D.A., Westberry, T.K., O'Brien, M.C., Nelson, N.B., Michaels, A.F., Morrison, J.R., Scott, A., Caporelli, E.A., Sorensen, J.C., Maritorena, S., Garver, S.A., Brody, E.A., Ubante, J., Hammer, M.A., 2001. Bio-optical modeling of primary production on regional scales: the Bermuda BioOptics Project. Deep-Sea Research II 48, 1865–1896.

Sorensen, J.C. and Siegel, D.A., 2001. Variability of the effective quantum yield for carbon assimilation in the Sargasso Sea. Deep-Sea Research II 48, 2005–2035.

Tanré, D., Deroo, C., Duhaut, P., Herman, M., Morcrette, J.J., Perbos, J., Deschamps, P.Y., 1990. Description of a computer code to simulate the satellite signal in the solar spectrum: the 5S code. International Journal of Remote Sensing 11, 659–668.

Venrick, E.L., 1971. Recurrent groups of diatom species in the North Pacific. Ecology 52, 614–625.

Venrick, E.L., 1990. Mesoscale patterns of chlorophyll *a* in the Central North Pacific. Deep-Sea Research 37, 1017–1031.

Venrick, E.L., 1993. Phytoplankton seasonality in the central North Pacific: the endless summer reconsidered. Limnology and Oceanography 38, 1135–1149.

Venrick, E.L., McGowan, J.A., Cayan, D.R., Hayward, T.L., 1987. Climate and chlorophyll *a*: Longterm trends in the central North Pacific Ocean. Fishery Bulletin 238, 70–72.

Waters, K.J., Smith, R.C., Marra, J., 1994. Phytoplankton production in the Sargasso Sea as determined using optical mooring data. Journal of Geophysical Research 99, 18 385–18 402.

Winn, C.D., Campbell, L., Christian, J.R., Letelier, R.M., Hebel, D.V., Dore, J.E., Fujieki, L., Karl, D.M., 1995. Seasonal variability on the phytoplankton community of the North Pacific Subtropical Gyre. Global Biogeochemical Cycles 9, 605–620.

Wright, S.W., Jeffrey, S.W., Mantoura, R.R.C., Llewellyn, C.A., Bjornland, T., Repeta, D., Welschmeyer, N., 1991. Improved HPLC method for the analysis of chlorophylls and carotenoids from marine phytoplankton. Marine Ecology Progress Series 77, 183–196.